Study on the characterization of filters for a direct-to-chip liquid cooling system

Pardeep Shahi[1], Ali Heydari[1], Himanshu Modi[2], Lochan Sai Reddy Chinthaparthy[2], Anto Barigala[2], Qusai Soud[1]
Uschas Chowdhury[1], Dereje Agonafer[2], Mohammad Tradat[1], Jeremy Rodriguez[1]
Nvidia[1], University of Texas at Arlington[2]
2788 San Tomas Expy
Santa Clara, CA, United States
pshahi@nvidia.com

Abstract

Data center cooling systems have undergone a major transformation in the persistent pursuit of better performance and lower energy use. Liquid cooling systems, particularly direct-to-chip systems, have emerged as a promising solution to address the increasing heat dissipation challenges. One critical component of such systems is the filtration mechanism, responsible for safeguarding the integrity and efficiency of the cooling process. These factors are pivotal in ensuring the reliable and sustainable operation of liquid cooling systems in high-demand applications, where electronic components continually push the boundaries of heat generation. This study undertakes a thorough examination of filters of different mesh size used in direct-to-chip liquid cooling systems. The research is multifaceted, encompassing the evaluation of filter performance, pressure drop characteristics, and long-term durability. The methodology employed in this research combines testing with a coolant distribution unit and rack setup to provide a holistic perspective on filter functionality. Findings from this study shed light on the key parameters that influence filter performance. Ultimately, the results of this research promise to contribute significantly to the advancement of direct-to-chip liquid cooling systems, facilitating the continued evolution of electronics in diverse fields, such as high-performance computing, data centers, and emerging technologies. With a focus on enhancing system reliability, efficiency, and sustainability, this study seeks to provide a valuable resource for engineers and researchers in the pursuit of effective cooling solutions for cutting-edge electronic applications.

Keywords

Filter, Coolant Distribution Units, CDU, Data Centers

1. Introduction

The relentless growth of data processing demands, propelled by technologies such as cloud computing, artificial intelligence, machine learning, and the Internet of Things, has made data centers indispensable in today's digital landscape. Demand for high-performance data centers has increased in the past decade and cooling high computing processors has become a major challenge [1]. To meet the ever-increasing computational needs, data centers have undergone significant transformations in cooling system design. Traditional air-based cooling systems struggle to dissipate the heat generated by today's powerful computers, necessitating the exploration of alternative cooling technologies. Liquid Cooling has been a promising solution as having a higher heat transfer coefficient than air cooling [2].

Much research has been conducted to improve the cooling performance via both air and liquid cooling approaches. For air cooling technology, studies have been conducted on hot/cold aisle containment [3][4], fan configurations [5], ducting at server level [6][7], indirect air-side economizer [8]. As with recent surge in requirement for high power dense chips due to rise in Artificial Intelligence (AI) and HPCs, cooling with air cooling becomes difficult to maintain the desired junction temperature, with higher chip density, more air flow rate and bigger heat sinks are required which increases the server form factor which in turn decreases the rack power density. Thus, for higher chip and rack density, microchannel-based liquid cooling is an excellent choice for a thermal solution as it provides a high heat transfer coefficient [9][10]. Research has been performed on improving the cooling via direct to chip liquid cooling. On cold plate level, the authors have developed an analytical model for top in/side exit (TISE), or split flow cold plate used in single phase cooling and studied the thermo-hydraulic performance of the cold plates by conducting experiments at various chip power [11][12]. The effects of inlet and outlet manifolds on the impingement microchannel cold plate hydraulic and thermal performance and with the CFD model they optimized the shape of the split flow cold plate [13-15]. A CFD model with hybrid cooling on a 1U server was used to study the coolant and air heat capture ratio and how factors like air and coolant input temperatures affect it [16]. An experimental study investigated the effect of a new duct designed to optimize the airflow and its effects on a hybrid cooled server [17]. Direct to Chip (D2C) cooling has gained significant popularity for the ease of use, low maintenance and retrofits, and flexibility of design changes. The D2C cooling technology uses rack manifolds, row manifolds or branches of tubes connecting cooling distribution units (CDUs), and pumps to circulate the primary and secondary loop coolant from the heat exchanger to the server. Heat exchangers such as L2A (Rear door [18][19], sidecar [20], in-row [21], [22], in-rack [23]) and L2L (in-rack [24], in-row [25]) are used to carry away the heat from the high heat server components to the CDU heat exchanger. At the heart of this cooling strategy lies the Coolant Distribution Unit, responsible for delivering coolant to heat-emitting components effectively and reliably. CDUs must dynamically adapt to changes in heat load, ensure uniform coolant distribution, and often incorporate filtration devices to maintain system reliability.

This research article focuses on a specific aspect of CDU operation—the filtration systems. Filtration plays a critical role in ensuring the delivery of clean liquid to sensitive electronic components while mitigating the ingress of particulate contaminants. The objectives of this comprehensive characterization study are Filter Performance Assessment, understanding the filter selection can also impact the pumping power. The insights gained are expected to contribute to the development of optimized filtration strategies, ultimately enhancing the efficiency, reliability, and sustainability of cooling distribution in data centers. Subsequent sections of this article will detail the methodology employed, present research findings, and discuss practical implications and recommendations within the context of data center operations.

2. Experimental Setup and Procedure

2.1. Experimental Setup

The experimental setup consists of a complex closed-loop system consisting of eight rack configurations. These setups are distinguished by carefully built row manifolds and rack manifolds. The rack configurations consist of many cooling loops, each designed to meet the individual requirements of various suppliers and are interconnected in a careful sequence. The central component of this intricate system is a coolant distribution unit equipped with a flat plate heat exchanger. The present module, in contrast, establishes a connection with a parallel configuration of variable frequency pumps, effectively coordinating the uninterrupted flow of the coolant. The CDU incorporates a diverse range of integrated sensors that function as a forefront mechanism for continuous monitoring in real-time. The sensors in question contain a range of key factors, including flow, temperature, and pressure. Additionally, supplemental pressure sensors are strategically placed throughout the filter units. The use of auxiliary sensors plays a crucial role in the identification and measurement of pressure variations experienced during the filtering process. These sensors serve as a valuable tool for assessing the level of cleanliness of the filter. Upon reaching a certain decrease in pressure, the sensors provide a signal, so triggering the requisite maintenance procedure of either cleaning or replacing the filter element. Figure 1 shows the used filtration system and sensors locations at a CDU level.

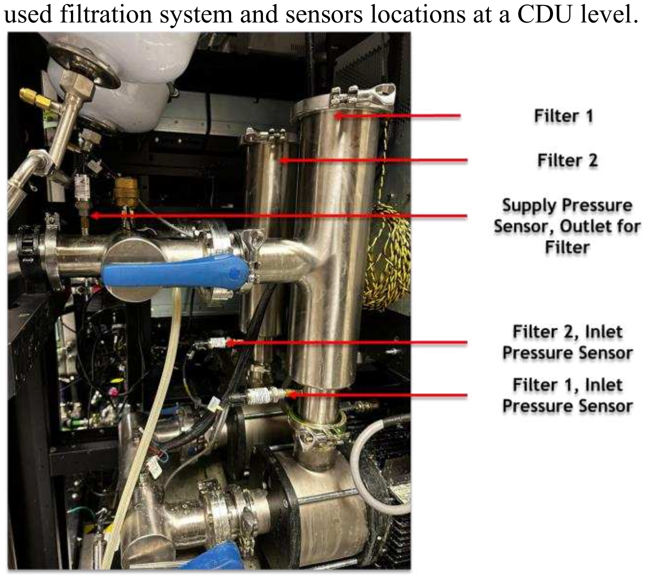

Figure 1: Internal of CDU

Furthermore, a very accurate inductive magnetic flow sensor is positioned on the supply side, namely between the row manifold and the CDU. This sensor is well-known for its exceptional precision. The inclusion of this sensor enhances the overall instrumentation system by offering an additional and validating means of measuring fluid flow rates. As a result, the timely identification and rectification of any disparities or abnormalities in the internal flow sensor of the CDU may effectively guarantee the accuracy and reliability of the acquired data. Temperature sensors, when combined with pressure sensors, play a crucial role in the supply, and return lines by carefully positioning them within the circuit, resulting in a harmonic integration of measurement and control. The sensors, located between the row manifold and the CDU, play a crucial role in collecting a complete dataset that is vital for assessing the thermal and hydraulic dynamics of the system. Figure 2 shows the schematic layout of the experimental setup.

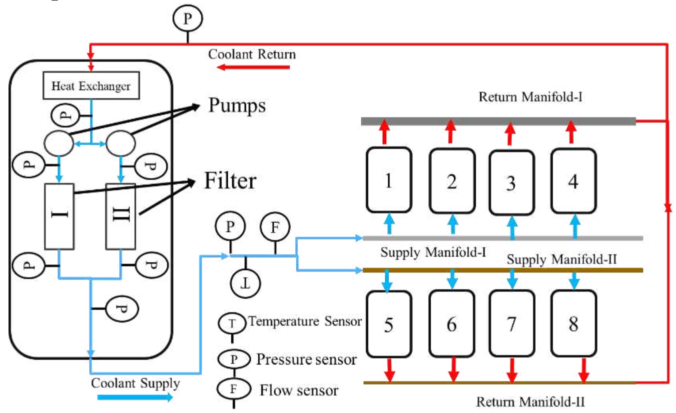

Figure 2: Schematic Layout of Experimental Setup

2.2. Design of the Experiments

The experimental design deals with filter size, pump dynamics, temperature gradients, and pressure differentials to demonstrate the parameters associated with coolant filtration process. The experimental approach correctly handles the coolant filtration variables of the central distribution unit. Three different filters were investigated 25, 50, and 100 µ m. additionally a critical control condition (no-filter situation) was incorporated to prove the results and adequately contrast the filter size impact.

To address pump dynamics, a variable frequency controller was used which allowed the pump to run at varying speed of 60%, 80% and 100%. The pump dynamics arrangement demonstrated how different flow rates affect filtration systems. These flow conditions were recorded for the various filters at inlet temperature of 32°C. In each instance, information was collected by measuring the pressure difference between the filter and the loop. Each situation is meticulously recorded, revealing the delicate relationship between filtration, temperature, and flow dynamics. Every statistic recorded is compared to a baseline, which represents the system dynamics with no-filter scenario.

2.3. Procedure

2.4. Creating a network arranging the cooling loops, rack manifold, row manifold, and CDU is the initial phase of this intricate study. The closed loop system is carefully filled with coolant. At modest flow rates, the CDU is optimized to maximize system performance. This step eliminates air bubbles and cavities from the circuit, resulting in a clean environment. A closed-loop system is then cleaned and maintained free of dust and debris using all available filter sizes**.** Afterward, the filters are cleaned using pressure washers to remove dust particles that have been collected. A final burst of compressed air is blown over the micron mesh to remove any fine particles still present. After ensuring all the debris is eliminated from the system a spare set of same sized filters are fitted into the slots. An inlet cover is used to close the filter slot and the system is filled with coolant to ensure a nominal pressure of 1.1 bar at idle. After thorough preparation, the system begins its temperature excursion. While the system operates at stable inlet temperatures, the key elements are recorded and logged. The data logging includes pressure differences between filter slots, pressure differences across the closed system, and flow rates throughout the system. This dataset served as the basis for all subsequent experiments**.** Both filter slots are fitted with filters of identical size during the course of the experiment.

At each stage of the process, the input temperature is carefully monitored, while the pump's speed is precisely regulated with the VFD to 60%, 80%, and 100%. Each instance of the logged data is meticulously and systematically documented. The results section discusses the collected data, the interaction between filter qualities, pump performance, and pressure dynamics after executing all three different filter sizes.

3. Results

3.1. Experiment 1: Entire System Connected

The pump speed was adjusted in this experiment between 20 and 100 percent for the studied cases no filter, 25µm, 50µm, and 100µm filter's size. The supply coolant temperature was maintained at 32 °C, the pressure drops across the filter was measured using pressure sensors located exactly at the inlet and outlet of the filter, Also, a well calibrated flow sensor used to report coolant flow rate at the outlet port of the CDU. Figure 3 shows the pressure drop across the filter at different pump speeds.

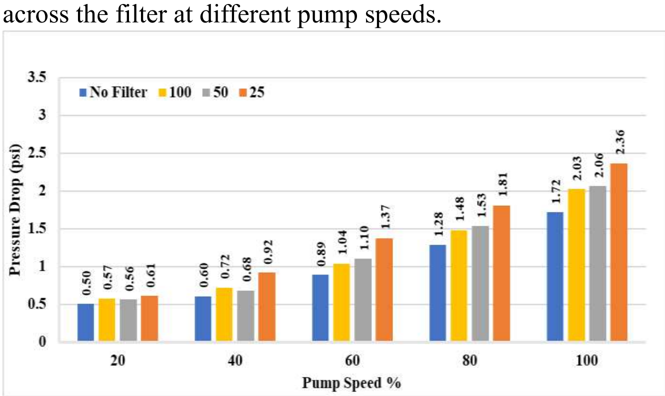

Figure 3: Pressure drop across the filter for variable pump speeds.

The graph in Figure 3 demonstrates that, under constant temperature conditions and with varying pump speeds, the maximum pressure loss is seen for 25-micron filters over the filter section, while the lowest pressure drop is recorded for without the presence of a filter. The no-filter situation was used as the baseline for typical operating circumstances at varied pump speeds.

At a minimum of 20% pump speed, the pressure drop difference between no filter and 25 Micron filter was about 0.11 Psi, increasing to 0.64 Psi at 100% pump speed. The pressure-drop readings for the 50 and 100-micron filters were almost identical to each other and fell between the baseline and the 25micron filter pressure drop.

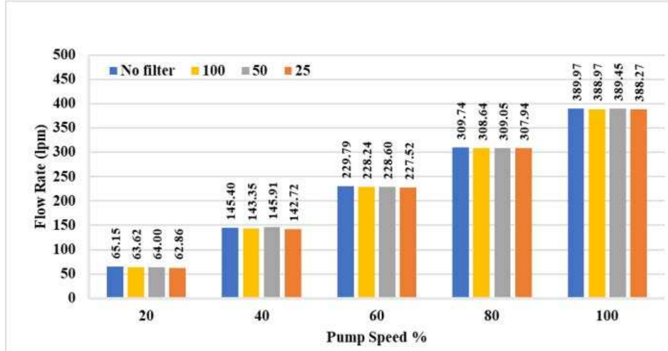

Figure 4: Coolant flow rate across the system for variable pump speeds

Changing the filter did not affect the flow rate throughout the system, as seen in Figure 4, which illustrates the relationship between flow rate and pump speed. The flow rate through the system with a 25-micron filter at maximum pump speed was measured to be 389 liters per minute (lpm). In comparison, when the system operated without any filter, the flow rate was 390 lpm, representing a mere 0.51% increase over the 25-micron filter with the finest mesh. At a pump speed of 80%, the absence of a filter resulted in the highest flow rate seen, which was 309.73 liters per minute (lpm). With 100- and 50-micron filters, the flow rate ranged from 308 to 309 lpm. For the 25-micron filter, the flow rate was 307.93 lpm. The flow rate exhibited a deviation of less than 1% in all cases for a certain pump speed, corresponding to a particular circumstance.

3.2. Experiment 2: System Reduced to 5 Racks

In this experiment, the total number of racks equipped with cooling loops and rack manifolds was reduced from eight to five. Furthermore, the remaining supply and return ports on the three racks were interconnected. As a result, the flow rates in the system increased due to the absence of pressure drop caused by the rack manifolds and cooling loops, which were impeding the flow.

The experiment was done with identical boundary conditions to experiment 1, with the exception that just the racks were shorted during this experiment.

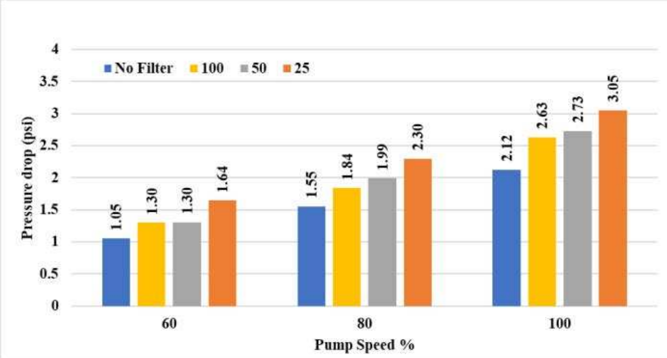

Figure 5: Pressure drop across the filter for variable pump speeds with five racks with TCS loops and three rack's supply and return ports interconnected.

The graphical representation from figure 5 illustrates that, across variable pump speeds of 60%, 80%, and 100%, the pressure drops were lowest when no filter was used, and highest when employing 25-micron filters. Comparing the no filter to the 25-micron filter case, a notable difference of approximately 0.93Psi, marking a 43.8% increase, was observed. The pressure drops for 50 and 100-micron filters fell between the extremes of no filter and the 25-micron filters, showing similar values. Additionally, a noticeable rise in pressure drops was evident when interconnecting three racks in contrast to eight interconnected racks.

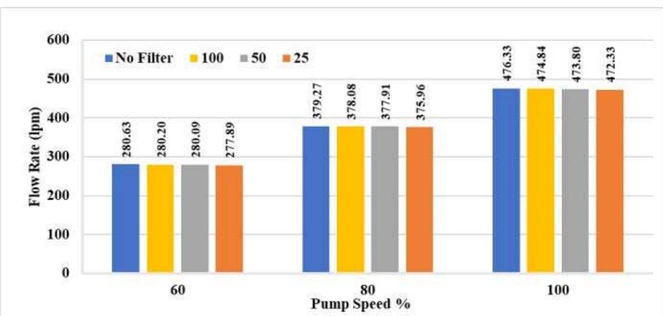

Figure 6: Flow rates across the system for variable pump speeds with five racks with TCS loops and three rack's supply and return ports interconnected.

The flow rates for all the filter scenarios with three racks interconnected seem to have an increase in values from the scenario with all the racks connected as shown in figure 6. At a maximum pump speed of 100% and with no filter in the slots, a peak flow rate of 476.33 liters per minute was noted. Introducing a 25 Micron filter at the same pump speed reduced the flow to approximately 472.33 lpm, a decline of around 4 liters per minute. Flow rates for both 50-micron and 100-micron filters exhibited comparable values, differing on average by only 1 lpm throughout the system. This consistency was observed across various pump speeds (60% and 80%) while maintaining a constant temperature of 32°C.

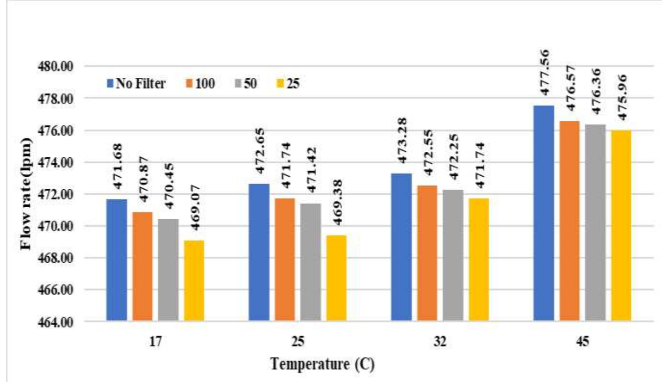

Figure 7: Flow rates across the system for constant pump speed at varying temperatures

Figure 7 shows the flow rate across the system for constant pump speed at varying temperature. Changes in coolant viscosity brought on by temperature variations were seen to cause variations in flow rates. For a constant pump speed of 100% and with varying temperatures shown in the figure we observed that at the lowest temperature of 17°C the no filter condition had a maximum flow rate of 471.68lpm and with the 25-micron filter condition the measured average flow rate was around 469.07lpm. Increasing the temperature to 45 C the no-filter condition has 477.56 lpm and with 25 Micron filter the measured flow rate was 475.96lpm. The temperature has a clear effect on the flow rates as the no filter condition had increased around 5.88lpm from 17ºC to 45ºC which is 1.24% similarly for the 25 micron filter the flow rates increased around 6.87 lpm from 17ºC to 45ºC which is 1.46% increase.

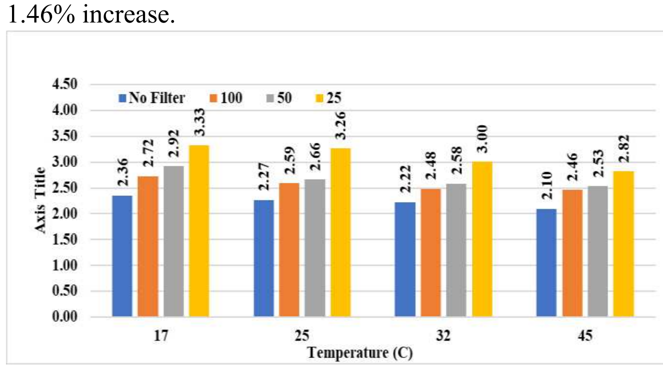

Figure 8: Flow rates across the system for constant pump speed at varying temperatures

The relationship between viscosity and pressure drop is significant in fluid dynamics, especially in the context of flow through conduits or systems. The bar graph from figure 8 illustrates how the pressure loss varies across filter slots at varying temperatures while keeping the pump speed at 100% constant. The pressure drop for the unfiltered condition was around 2.36 psi at the lowest temperature (17°C), and it decreased to 2.1 psi at 45°C, indicating an 11% reduction. Comparably, to the 25-micron filter, the observed pressure at 17°C was 3.33 psi at first, but at 45°C, it dropped to 2.82 psi, indicating a 14% reduction. This pattern suggests a discernible effect on system performance as temperatures increase by showing a consistent decrease in pressure drop throughout the filter slots with rising temperatures.

4. Conclusion

Experiments in the research revealed significant insights on pressure decreases and flow rates under a variety of system circumstances. At 100% pump speed, pressure decreases across filter slots were measured in the first experiment. The lowest pressure reduction was seen when no filter was present, whereas finer filters (25, 50, and 100 micron) showed a constant increase in pressure. The flow rate, on the other hand, stayed relatively constant with very little variations—less than 1%—across a range of pump speeds, highlighting the influence of pump speed and filter size on pressure decreases rather than flow rate.

In the second experiment, reducing and interconnecting the linked racks showed a similar pattern of pressure losses, with the biggest pressure drops for 25-micron filters and the lowest for no filters. Flow rates were affected by temperature variations, showing observable increases as temperatures rose.

The bar graphs clearly showed the link between temperature with coolant flow rates and pressure drop, showing consistently lower pressure drops at higher temperatures. At 45°C, the decreases were 11% and 14% for the no-filter and 25-micron cases, respectively. These results highlight how temperature has a major impact on the system's operation.

References

1. Y. Hadad, S. Rangararajan, K. Nemati, B. Ramakrishnann, R. Pejman, P. R. Chiarot, B. Sammakia,, "Performance analysis and shape optimization of a water-cooled impingement micro-channel heat sink including manifolds," International Journal of Thermal Sciences, vol. 148, no. ISSN 1290-0729, p. 106145, 2020.
2. R. Schmidt, "Packaging of new servers-energy efficiency aspects," in Proc. 1st Berkeley Symp. Energy Efficient Electron., Berkeley, CA, USA, Jun. 2009, pp. 1–35. [Online]. Available: https://e3s-center.berkeley.edu/wp-content/uploads/2017/07/RogerSchmidt.pdf
3. Zhou, Rongliang, Zhikui Wang, Cullen E. Bash, and Alan McReynolds. "Modeling and control for cooling management of data centers with hot aisle containment." In ASME International Mechanical Engineering Congress and Exposition, vol. 54907, pp. 739-746. 2011.
4. Schmidt, Roger, Aparna Vallury, and Madhusudan Iyengar. "Energy savings through hot and cold aisle containment configurations for air cooled servers in data centers." In International Electronic Packaging Technical Conference and Exhibition, vol. 44625, pp. 611-616. 2011.
5. Shigrekar, Neha. "Quantifying Air Flow Rate Through A Server In An Operational Data Center And Assessing The Impact Of Using Theoretical Fan Curve." (2015).
6. Modi, Himanshu, Uschas Chowdhury, and Dereje Agonafer. "Impact of Improved Ducting and Chassis Re-design for Air-Cooled Servers in a Data Center." In 2022 21st IEEE Intersociety Conference on Thermal and Thermomechanical Phenomena in Electronic Systems (iTherm), pp. 1-8. IEEE, 2022.
7. Zhou, David, Ming Zhang, and Chris Du. "Enhancing rack servers air cooling capability with extra system inlet airflow through air ducts between racks." In 2017 16th IEEE Intersociety Conference on Thermal and Thermomechanical Phenomena in Electronic Systems (ITherm), pp. 857-863. IEEE, 2017.
8. Iyengar, Madhusudan, Roger Schmidt, Vinod Kamath, and Prabjit Singh. "Energy efficient economizer based data centers with air cooled servers." In 13th InterSociety Conference on Thermal and Thermomechanical Phenomena in Electronic Systems, pp. 367-376. IEEE, 2012.
9. Incropera, F., Liquid Cooling of Electronic Devices by Single-Phase Convection, John Wiley & Sons (New York, 1999), pp. 125-163.
10. S. V. Garimella & V. Singhal (2004) Single-Phase Flow and Heat Transport and Pumping Considerations in Microchannel Heat Sinks, Heat Transfer Engineering, 25:1, 15-25, DOI: 10.1080/01457630490248241
11. V. Torreblanca, A. Soto and D. Kulkarni, 2019, "Design and Testing of Liquid Cooled Thermal Solution for High Loading Processors," 18th IEEE Intersociety Conference on Thermal and Thermomechanical Phenomena in Electronic Systems (ITherm), Las Vegas, NV, USA, 2019, pp. 965-975. doi: 10.1109/ITHERM.2019.8757362
12. Kisitu, Deogratius, and Alfonso Ortega. "Thermal-Hydraulic Analytical Models of Split-Flow Microchannel Liquid-Cooled Cold Plates With Flow Impingement." In International Electronic Packaging Technical Conference and Exhibition, vol. 85505, p. V001T02A015. American Society of Mechanical Engineers, 2021.
13. Ramakrishnan, B., Hadad, Y., Alkharabsheh, S., Chiarot, P. R., and Sammakia, B. (July 12, 2019). "Thermal Analysis of Cold Plate for Direct Liquid Cooling of High Performance Servers." ASME. J. Electron. Packag. December 2019; 141(4): 041005. https://doi.org/10.1115/1.4044130.
14. Gharaibeh, Ahmad R., Yaman M. Manaserh, Mohammad I. Tradat, Firas W. AlShatnawi, Scott N. Schiffres, and Bahgat G. Sammakia. "Using a Multi-Inlet/Outlet Manifold to Improve Heat Transfer and Flow Distribution of a Pin Fin Heat Sink." Journal of Electronic Packaging 144, no. 3 (2022): 031017.
15. Gharaibeh, Ahmad R., Mohammad I. Tradat, Srikanth Rangarajan, Bahgat G. Sammakia, and Husam A. Alissa. "Multi-objective optimization of 3D printed liquid cooled heat sink with guide vanes for targeting hotspots in high heat flux electronics." International Journal of Heat and Mass Transfer 184 (2022): 122287.
16. Shalom Simon, V, Reddy, LS, Shahi, P, Valli, A, Saini, S, Modi, H, Bansode, P, & Agonafer, D. "CFD Analysis of Heat Capture Ratio in a Hybrid Cooled Server." Proceedings of the ASME 2022 International Technical Conference and Exhibition on Packaging and Integration of Electronic and Photonic Microsystems. ASME 2022 International Technical Conference and Exhibition on Packaging and Integration of Electronic and Photonic Microsystems. Garden Grove, California, USA. October 25–27, 2022. V001T01A013. ASME. https://doi.org/10.1115/IPACK2022-97445

17. Modi, Himanshu, Pardeep Shahi, Lochan Sai Reddy Chinthaparthy, Gautam Gupta, Pratik Bansode, Vibin Shalom Simon, and Dereje Agonafer. "Experimental Investigation of the Impact of Improved Ducting and Chassis Re-Design of a Hybrid-Cooled Server." In International Electronic Packaging Technical Conference and Exhibition, vol. 86557, p. V001T01A019. American Society of Mechanical Engineers, 2022.
18. M. J. Ellsworth, L. A. Campbell, R. E. Simons, M. K. Iyengar, R. R. Schmidt, and R. C. Chu, “The evolution of water cooling for IBM large server systems: Back to the future,” in 2008 11th Intersociety Conference on Thermal and Thermomechanical Phenomena in Electronic Systems, May 2008, pp. 266–274, doi: 10.1109/ITHERM.2008.4544279.
19. Shalom Simon, Vibin, Himanshu Modi, Krishna Bhavana Sivaraju, Pratik Bansode, Satyam Saini, Pardeep Shahi, Saket Karajgikar, Veerendra Mulay, and Dereje Agonafer. "Feasibility Study of Rear Door Heat Exchanger for a High Capacity Data Center." In International Electronic Packaging Technical Conference and Exhibition, vol. 86557, p. V001T01A018. American Society of Mechanical Engineers, 2022.
20. R. Schmidt, M. Iyengar, D. Porter, G. Weber, D. Graybill, and J. Steffes, “Open side car heat exchanger that removes entire server heat load without any added fan power,” in 2010 12th IEEE Intersociety Conference on Thermal and Thermomechanical Phenomena in Electronic Systems, Jun. 2010, pp. 1–6, doi: 10.1109/ITHERM.2010.5501423.
21. U. Chowdhury, W. Hendrix, T. Craft, W. James, A. Sutaria, and D. Agonafer, “Optimal Design and Modeling of Server Cabinets With In-Row Coolers and Air Conditioning Units in a Modular Data Center,” in ASME 2019 International Technical Conference and Exhibition on Packaging and Integration of Electronic and Photonic Microsystems, Anaheim, California, USA, Oct. 2019, p. V001T02A009, doi: 10.1115/IPACK2019-6522.
22. T. Gao, B. G. Sammakia, J. Geer, B. Murray, R. Tipton, and R. Schmidt, “Comparative Analysis of Different In Row Cooler Management Configurations in a Hybrid Cooling Data Center,” in Volume 1: Thermal Management, San Francisco, California, USA, Jul. 2015, p. V001T09A011, doi: 10.1115/IPACK2015-48069.
23. T. Gao et al., “Innovative server rack design with bottom located cooling unit,” in 2016 15th IEEE Intersociety Conference on Thermal and Thermomechanical Phenomena in Electronic Systems (ITherm), May 2016, pp. 1172–1181, doi: 10.1109/ITHERM.2016.7517681.
24. H. Coles, S. Greenberg, and P. Hughes, “Rack-Level Cooling and Cold Plate Cooling,” in Data Center Handbook, John Wiley & Sons, Ltd, 2014, pp. 479–493.
25. M. J. Ellsworth, G. F. Goth, R. J. Zoodsma, A. Arvelo, L. A. Campbell, and W. J. Anderl, “An Overview of the IBM Power 775 Supercomputer Water Cooling System,” Journal of Electronic Packaging, vol. 134, no. 2, p. 020906, Jun. 2012, doi: 10.1115/1.4006140.